Asian Journal of Chemistry; Vol. 30, No. 7 (2018), 1650-1654

ASIAN JOURNAL OF CHEMISTRY

https://doi.org/10.14233/ajchem.2018.21425

Synthesis, Characterization and Catalytic Activity of NiO-Mn_2O_3/ZrO_2 Spinel Co-Catalysts

SALIH HADI KADHIM

Department of Chemistry, College of Science, University of Babylon, Hilla 51002, Iraq

Corresponding author: E-mail: hadi197019@yahoo.com

Received: 5 May 2018; *Accepted*: 30 May 2018; *Published online*: 31 May 2018; AJC-18948

The spinel co-catalyst NiO-Mn_2O_3/ZnO_2 in two different ratios (0.5:0.5:2) and (1:2:1) of the components oxides were prepared using co-precipitation method of their metal hydroxides. This method was performed in basic medium (pH 9), using sodium carbonate as a precipitated agent. The precipitated samples dried at 120 ºC overnight and then calcinated at 650 ºC for three hours. The prepared spinel co-catalyst was investigated using powder X-ray diffraction, Fourier transfer infrared spectroscopy, energy-dispersive X-ray spectroscopy and atomic force microscopy. According to spectroscopic studies and magnetic properties, the obtained co-catalyst was a normal spinel type. The catalytic activity of prepared co-catalysts was conducted by following photocatalytic degradation of Bismarck Brown G dye. From the obtained results, the best ratio of spinel catalyst was (0.5:0.5:2) optimized, which achieved a higher activity for removal percentage (97 %) dye.

Keywords: Spinel catalyst, NiO-Mn_2O_3/ZrO_2 catalyst, Spinel oxide.

INTRODUCTION

The spinel oxide structure containing two oxidation states of metal ion M^{2+} and M^{3+} in the general formula $(A^{2+})(B^{3+})_2O_4$, AB_2O_4 or $AO.B_2O_3$. The metal ion with large size tends to prefer the tetrahedral site and the metal ion with the smallest size tend to prefer octahedral site [1,2], such as spinel catalyst $SrAl_2O_4$, $ZnFe_3O_4$ [3,4]. In these oxides, Sr and Zn as a larger divalent ions occupy the tetrahedral sites while Al and Fe as a smallest trivalent ions occupy the octahedral sites in spinel oxides structure. Oxides of transition metals can be used as a catalyst in wide range of industrial applications because of their electronic and magnetic properties. In this context, nickel, manganese oxides are among of these oxide are used as catalysts in different types of industrial applications [5,6]. Nickel oxide considers a p-type semiconductor and is used as a catalyst in a wide range of environ-mental applications because of their electrical properties [7,8]. Mn_2O_3 found in a cubic structure and consider as an effective transition metal oxide in catalyst components [9] and used as a catalyst in a wide range of applications in wastewater treatments such as reduction of nitrous oxide and oxidation and decom-position of the methylene blue dye with H_2O_2 [10-12]. The binary spinel oxides $NiMn_2O_4$ shows a cubic spinel structure [13].

Zirconium oxide has a defect structure in which oxygen ion occupy the vacancy that is surrounded by all metal ions in there lattice point. In this case, each oxygen ion is surrounded by four zirconium ions to form a tetrahedral structure and each zirconium ion is surrounded by eight oxygen ion forming the body centered cubic structure [14-16]. The present study describes the synthesis of spinel co-catalyst NiO-Mn_2O_3/ZrO_2 *via* co-precipitation method and its good catalytic applications in the decolorization of Bismarck Brown G.

EXPERIMENTAL

In present investigations, $Mn(CH_3COO)_2{\cdot}4H_2O$, $Ni(NO_3)_2{\cdot}6H_2O$ and $ZrCl_4$ were procured from BDH company with purity was 98, 99.9 and 98 %, respectively. Anhydrous sodium carbonate obtained from GmbH company with purity 99.9 %. Bismarck Brown G, an azo disperse dye with molecular formula $C_{18}H_{18}N_8{\cdot}2HCl$ is obtained from Hilla Textile Factory, Babylon, Iraq.

Synthesis of catalyst: NiO-Mn_2O_3 in different ratios (0.5:0.5) and (1:2) were prepared by coprecipitation method, while supported catalyst NiO-Mn_2O_3/ZrO_2 was prepared by wet impregnation method having zirconium carbonate in ratios 30 % of (0.5:0.5) NiO-Mn_2O_3 to 70 % ZrO_2 (**catalyst 1**) and 70 % of (1:2) NiO-Mn_2O_3 to 30 % of ZrO_2 (**catalyst 2**) from their primary materials, $Ni(NO_3)_2{\cdot}6H_2O$, $Mn(CH_3COO)_2{\cdot}4H_2O$ and $ZrCl_4$. Weighed accurately amount of these ratios were dissolved in 300 mL of deionized water and added 1 M Na_2CO_3 as a precipitating agent until pH of mixture reached to 9, the adjustment of pH by using a digital pH meter (type 740 Inolab WTW, Germany), with stirring and heated at 70-75 ºC. The mixture was then left for 2 h at the same reaction temperature with stirring

to complete the digestion process. Then the mixture was filtered, washed carefully with deionized water and dried in an oven for overnight at 120 ºC. The resulting precipitate was calcinated at 650 ºC for 3 h with heating rate at 10 ºC/min in a muffle furnace type (Size-Tow Gallenkamp, England).

Powder X-ray diffraction: The crystalline phase patterns for the mixed oxides in the prepared co-catalysts was investigated using powder X-ray diffractometer type Siemens D500 with a CuK_α X-ray source (1.5418 Å). The working voltage and current for X-ray was 40 kV and 40 mA, respectively. The scan range of 2θ = 10-80º. The energy-dispersive X-ray spectroscopy (EDX) was used to determine the purity and elemental percentage in the prepared co-catalyst.

Fourier transform infrared spectroscopy: Perkin Elmer Company, England was used to analyze the functional groups of mixed oxides in the prepared catalyst. The spectra were recorded in the range of wavenumbers from 4000-400 cm^{-1}.

Atomic force microscopy: Atomic force microscopy type SPM-AA3000 Atomic Force Microscope 2005 (USA) was used to study the surface morphology of mixed oxides in their different ratios in the prepared catalyst.

Photocatalytic removal of Bismarck Brown G dye over prepared co-catalysts: A series of experiments were performed to remove Bismarck Brown G dye from textile and effluents using NiO-Mn_2O_3, co-catalyst 1 and co-catalyst 2 to investigate their catalytic activity and choose the best one. All the experiments were performed by adding 0.025 g of catalyst into the reaction cell (Fig. 1). This contains dye solution (100 ppm, 30 mL) of Bismarck Brown G dye. The reaction mixture was carried out at a constant temperature (298 K). Irradiation of reaction mixture was performed using mercury vapor lamp (250 W) supplied from (Philips company, Holland) use as a source of UV radiation in the reaction and initiated after 10 min of dark reaction. After 20 min, 2 mL of reaction samples was withdrawn and centrifuged carefully. Then the absorbances were recorded at 431 nm for Bismarck Brown G dye using UV-visible spectrophotometer (Shimadzu 1100A, Japan).

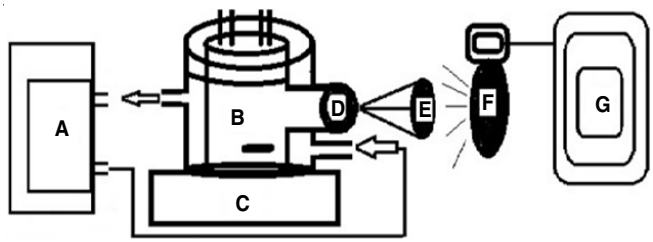

(A) Circulator water bath
(B) Reaction cell
(C) Magnetic stirrer
(D) Quartz window
(E) Lens
(F) Low pressure lamp
(G) Power supply unit

Fig. 1. Homemade unit of photocatalytic reaction

Effect of doses of catalyst 1 in photocatalytic removal of Bismarck Brown G dye: The dose effect of the prepared catalyst (**co-catalyst 1**) was investigated by using different weight (0.025, 0.05, 0.075, 0.2, 0.125 and 0.15 g) in order to determine the optimum amount which would show a maximum removal of Bismarck Brown G dye after a contact period of 20 min for the photocatalytic reaction.

RESULTS AND DISCUSSION

X-Ray diffraction: Crystal structure of the prepared co-catalyst was investigated using XRD patterns. Different peaks of crystal structure at different diffraction angles and miller indices (hkl) were recorded. The peaks at 37.3º (111), 43.5º (200), 63.3º (220) and 75º (311) refer to formation of NiO in cubic spinel structure [17]. Other peaks at 23.1º , 32.9º, 37º, 55.5º, 65.8 corres-pond to the crystalline planes (211), (222), (400), (440) and (622) of Mn_2O_3 (Fig. 2). When matched of these data with JCPDS file card No: 47-1049 and card no. 00-001-1110, it can be concluded that the formation of cubic spinel structure of NiO-Mn_2O_3 in binary and ternary spinel catalyst. The main peaks of XRD for ZrO_2 at diffraction angles (2θ) and miller indexes equal to 30.5º (111), 35.193º (200) and 50.68º (220) referred to the formation of tetragonal phase of ZrO_2. The average particle size of NiO-Mn_2O_3, co-catalyst 1 and co-catalyst 2 equal to 10.25, 11.23 and 39.97 nm, respectively as estimated using Debye-Scherer's equation.

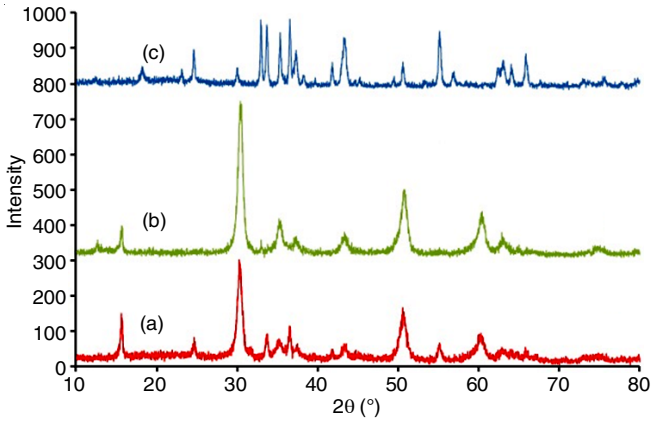

Fig. 2. PXRD patterns of (a) co-catalyst 1, (b) co-catalyst 2 and (c) NiO-Mn_2O_3

The EDX analyses of the prepared catalysts showed intense peaks corresponding only for Ni, Mn, O and Zr, and determined the elemental percentage in these catalysts of nickel (20 %), manganese (27 %), oxygen (25.6 %) and zirconium (23 %) which was in the excellent similarity with the calculated values as shown in Figs. 3 and 4.

FT-IR studies: The infrared spectra of co-catalyst 1, co-catalyst 2 and NiO-Mn_2O_3 are shown in Fig. 5. The appearance of stretching vibrations in the region of 478 and 430 cm^{-1}, corresponds to Ni-O bonds [18]. The absorption peaks at 526 and 607

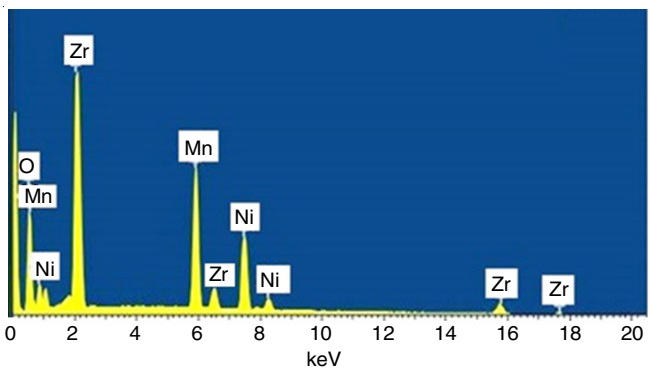

Fig. 3. EDX analysis of co-catalyst 1

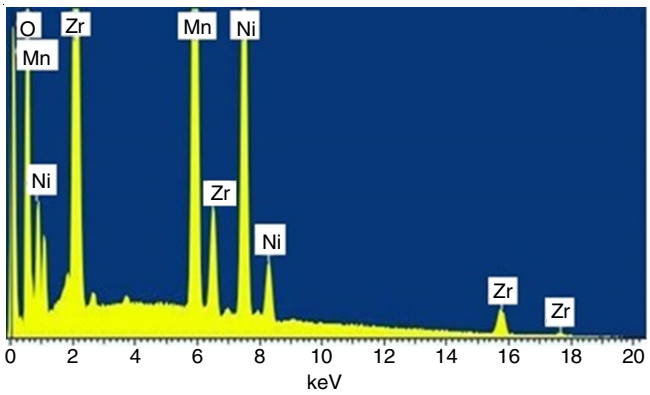

Fig. 4. EDX analysis of co-catalyst 2

cm^{-1} are due to the vibrational bands of Mn-O and Mn-O-Mn, respectively [19], while the vibration bands for Zr-O [20] at 461, 578 and 744 cm^{-1}. The stretching band of O-H group at 3400 and 1650 cm^{-1} corresponded to the surface adsorbed water and hydroxyl groups, respectively [21-23].

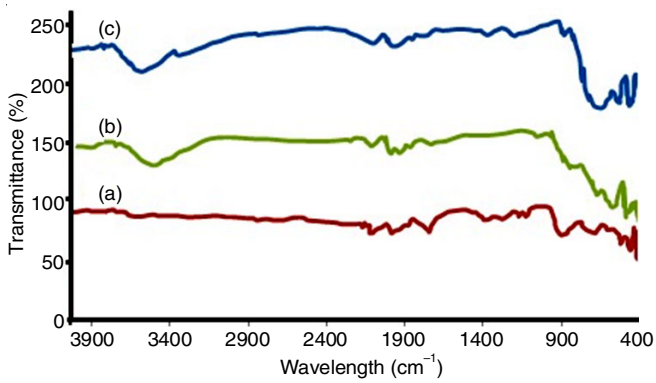

Fig. 5. FT-IR spectra of (a) co-catalyst 1 (b) co-catalyst 2 and (c) NiO-Mn_2O_3

Atomic force microscopy of prepared co-catayst: The morphological images of co-catalyst 1 , co-catalyst 2 and NiO-Mn_2O_3 surface are shown in Figs. 6-8. The particles size of molecules and its distribution on the surface was equal to 63.6, 72.9 and 89.4 nm for the catalyst, respectively. This arrangement in the crystal size is agreement with the arrangement that was calculated from Debye Scherer equation. From these results one can concluded that co-catalyst 1 exhibited a best morphological surfaces and smallest particle size, while the other ratio and dual oxide spinel gives large particles size. All these particle size which lie in the meso region will be efficient and can improve catalytic activity of the used catalyst [24].

Magnetic properties of prepared co-catalysts: The magnetic moments of prepared co-catalysts were calculated by measuring the magnetic susceptibility using Faraday method with Balance Magnetic Susceptibility Model-M-S-Auto.

Catalytic activity of prepared co-catalysts: The catalytic activity of the prepared materials was investigated by removal of Bismarck brown G dye from its aqueous solution by adsorption and photocatalytic reactions. This was performed by using 0.025 g of prepared NiO-Mn_2O_3, co-catalyst 1 and co-catalyst 2. The obtained results showed that the best activity in dye removal was found to be for catalyst 1 after 20 min of processing of reaction mixture (Table-1). This co-catalyst

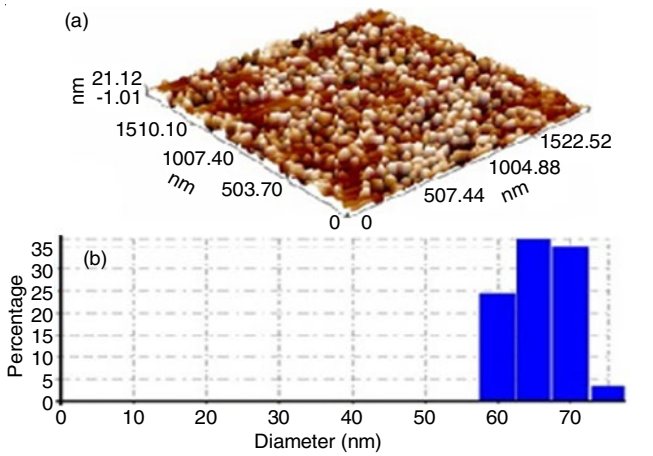

Fig. 6. Atomic force microscopy of co-catalyst 1 (a) granularity cumulation distribution chart (b) image of surface

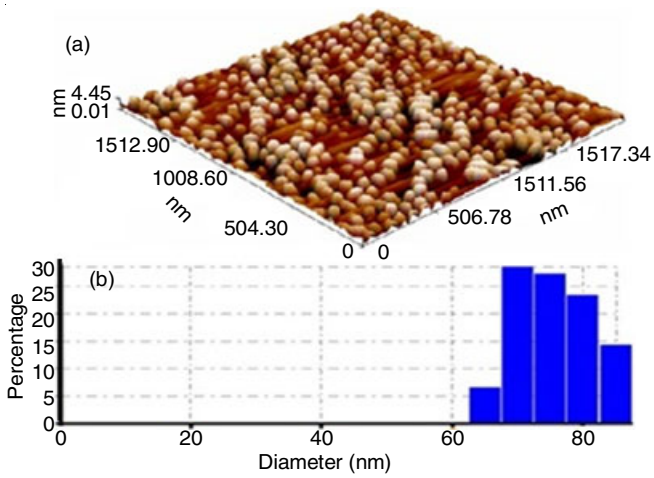

Fig. 7. Atomic force microscopy of co-catalyst 2 (a) granularity cumulation distribution chart (b) image of surface

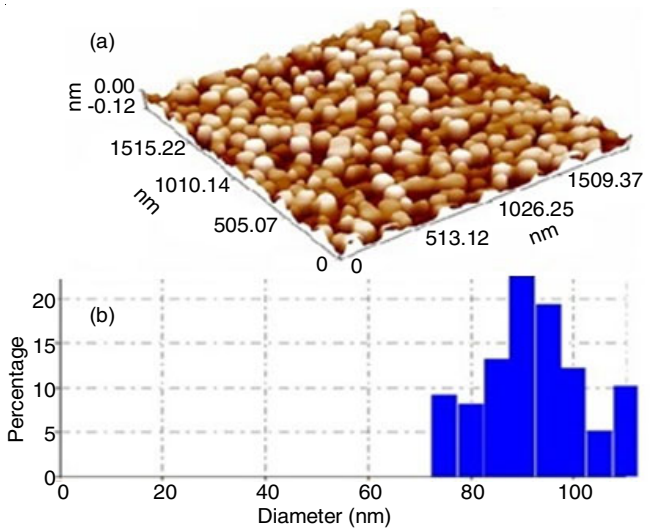

Fig. 8. Atomic force microscopy of NiO-Mn_2O_3 (a) granularity cumulation distribution chart (b) image of surface

exhibited maximum removal percentage which was found to be 91 %.

Effect of mass dosage of catalyst 1 on photocatalytic removal of Bismarck Brown G dye: Fig. 9 shows the best optimum mass dosage of catalyst 1 was 0.05 g. which shows a

TABLE-1
REMOVAL EFFICIENCY OF BISMARCK BROWN G DYE OVER SINGLE, DUAL AND TERNARY OXIDES

Absorbance of dye = 4.5330; λ = 431 nm; t = 0 without catalyst		
Catalyst	Absorbance of dye	Removal of dye (%)
Mn_2O_3	1.7580	61
NiO-Mn_2O_3	0.9150	80
Co-catalyst 2	0.4978	89
Co-catalyst 1	0.4173	97

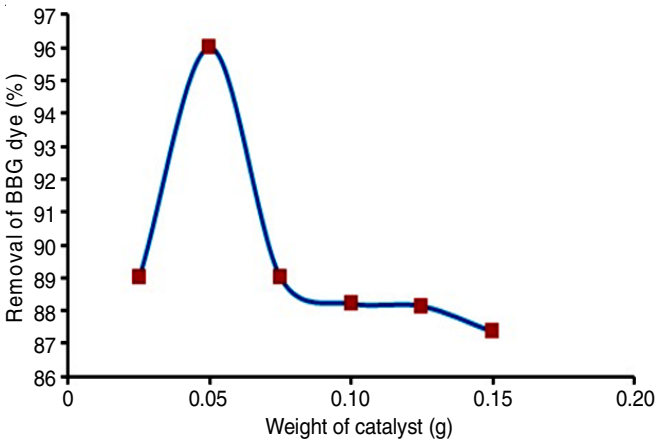

Fig. 9. Removal of Bismarck Brown G dye over different doses of co-catalyst 1

high removal efficiency of the Bismarck Brown G (97 %) over the prepared co-catalyst 1 after 20 min of initiation of photoreaction over the used catalyst.

Removal efficiency of the dye increases with increase of catalyst doses from 0.025 to 0.05 g and then it was decreased from 0.075 to 0.15 g. This is due to the increase of active sites numbers on the surface of the catalyst for the photoreaction and then after weight 0.075 g the removal efficiency decreased. This is due to increased concentration of the catalyst and increase the turbidity of the solution which works to reflect the light, and reduce the number of photons entering to internal solution, therefore decreases the number of surface active sites [25,26], hence, the most effective photodegradation of Bismarck Brown G was observed with 0.05 g of catalyst weight.

Suggested structure of spinel co-catalyst: From crystal field stabilization energy (CFSE) calculations, it can be concluded to investigate the type of spinel structure. The co-catalyst 1 is found to be a normal spinel because of trivalent manganese, which have a higher CFSE, and consequently has a smallest ion size as compared to divalent nickel. Therefore, Ni^{2+} occupy tetrahedral site and Mn^{3+} occupied the octahedral site in cubic spinel structure [2,27,28]. From the comparison data between experimental and theoretical magnetic moments values, it further confirmed the normal spinel oxide structure AB_2O_4 of co-catalyst 1.The net magnetic moment equal to the difference between magnetic moments at A and at B sites in $A^{\rightarrow}[^{\leftarrow}B\ ^{\leftarrow}B]O_4$. The magnetic moment for two B(Mn^{3+}) are parallel to those at all the B sites and antiparallel to those at all the A(Ni^{2+}) sites, therefore $\mu = 2\mu_B - \mu_A = 2(4.89) - 2.83 = 6.97$ B.M., this value is well in agreement with the experimental value, which equal to 5.72 B.M. [29]. Finally from all these results and spectrometric studies, it can be suggested a normal spinel structure for the prepared co-catalyst as shown in Fig. 10.

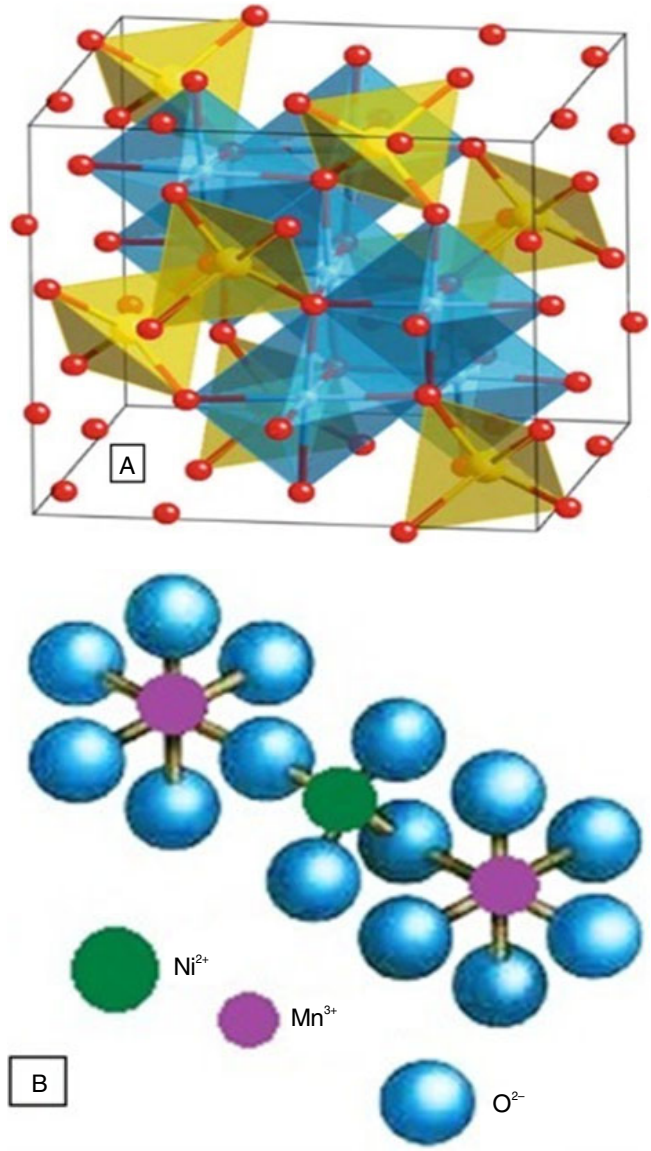

Fig. 10. Spinel structure of catalyst: A-cubic spinel, blue in octahedral unit, yellow in tetrahedral unit, red sphere represents oxygen ion B-section from cubic spinel

Conclusion

The spinel co-catalysts NiO-Mn_2O_3/ZnO_2 in two different ratios (0.5:0.5:2) and (1:2:1) of the components oxides were prepared by co-precipitation method. The prepared spinal materials are also evaluatied for ther catalytic activity for the removal of Bismarck Brown G dye from the effluents of textile wastewater. The best ratio of the prepared catalyst NiO-Mn_2O_3/ZnO_2 was 30 % from (0.5:0.5) NiO-Mn_2O_3:70 % of ZrO_2 having a normal spinel structure in cubic system. This co-catalyst exhibited high catalytic activity for removal of Bismarck Brown G dye which was around 97 % in a contact period of 20 min.

REFERENCES

1. M. Sugawara, M. Ohno and K. Matsuki, *J. Mater. Chem.*, **7**, 833 (1997); https://doi.org/10.1039/a607324g.
2. H. St. C. O'Neill and A. Navrotsky, *Am. Miner.*, **68**, 181 (1983).
3. P. Mierczynski, K.A. Chalupka, W. Maniukiewicz, I.S. Malgorzata, J. Kubicki and T.P. Maniecki, *Appl. Catal. B: Environ.*, **164**, 176 (2015); https://doi.org/10.1016/j.apcatb.2014.09.003.

4. T.M. Sankaranarayanan, K. Thirunavukkarasu, A. Pandurangan, R.V. Shanthi and S. Sivasanker, *J. Mol. Catal. A*, **379**, 234 (2013); https://doi.org/10.1016/j.molcata.2013.08.027.
5. T. Hyeon, *Chem. Commun.*, 927 (2003); https://doi.org/10.1039/b207789b.
6. L. Daza, C.M. Rangel, J. Baranda, M.T. Casais, M.J. Martínez and J.A. Alonso, *J. Power Sources*, **86**, 329 (2000); https://doi.org/10.1016/S0378-7753(99)00499-1.
7. N.R. Jana, Y.F. Chen and X.G. Peng, *Chem. Mater.*, **16**, 3931 (2004); https://doi.org/10.1021/cm049221k.
8. Y. Wang, J. Zhu, X. Yang, L. Lu and X. Wang, *Thermochim. Acta*, **437**, 106 (2005); https://doi.org/10.1016/j.tca.2005.06.027.
9. M.C. Álvarez-Galván, V.A. de la Peña O'Shea, J.L.G. Fierro and P.L. Arias, *Catal. Commun.*, **4**, 223 (2003); https://doi.org/10.1016/S1566-7367(03)00037-2.
10. J. Cao, Q. Mao and Y. Qian, *J. Solid State Chem.*, **191**, 10 (2012); https://doi.org/10.1016/j.jssc.2012.02.061.
11. G. Fierro, M. Lo Jacono, M. Inversi, R. Dragone and G. Ferraris, *Appl. Catal. B*, **30**, 173 (2001); https://doi.org/10.1016/S0926-3373(00)00232-0.
12. Z. Yang, Y. Zhang, W. Zhang, X. Wang, Y. Qian, X. Wen and S. Yang, *J. Solid State Chem.*, **179**, 679 (2006); https://doi.org/10.1016/j.jssc.2005.11.028.
13. G.D.C.C. de Györgyfalva and I.M. Reaney, *J. Mater. Res.*, **18**, 1301 (2003); https://doi.org/10.1557/JMR.2003.0179.
14. A.F. Wells, *Solid State Phys*., **7**, 425 (1958); https://doi.org/10.1016/S0081-1947(08)60556-1.
15. S. Shukla, S. Seal, R. Vij, S. Bandyopadhyay and Z. Rahman, *Nano Lett.*, **2**, 989 (2002); https://doi.org/10.1021/nl025660b.
16. N. Igawa and Y. Ishii, *J. Am. Ceram. Soc.*, **84**, 1169 (2001); https://doi.org/10.1111/j.1151-2916.2001.tb00808.x.
17. H. Qiao, N. Wu, F. Huang, Y. Cai and Q. Wei, *Mater. Lett.*, **64**, 1022 (2010); https://doi.org/10.1016/j.matlet.2010.01.037.
18. K.S. Pugazhvadivu, K. Ramachandran and K. Tamilarasan, *Phys. Procedia*, **49**, 205 (2013); https://doi.org/10.1016/j.phpro.2013.10.028.
19. H. Chen and J. He, *J. Phys. Chem. C*, **112**, 17540 (2008); https://doi.org/10.1021/jp806160g.
20. R. Arreche, N. Bellotti, M. Blanco and P. Vázquez, *Procedia Mater. Sci.*, **9**, 627 (2015); https://doi.org/10.1016/j.mspro.2015.05.039.
21. D. Khushalani, G.A. Ozin and A. Kuperman, *J. Mater. Chem.*, **9**, 1491 (1999); https://doi.org/10.1039/a902291k.
22. G.J. Li and S. Kawi, *Talanta*, **45**, 759 (1998); https://doi.org/10.1016/S0039-9140(97)00295-6.
23. Y.-L. Song, J.-T. Li and B. Bai, *Water Air Soil Pollut.*, **213**, 311 (2010); https://doi.org/10.1007/s11270-010-0386-0.
24. C. Contreras, F. Isquierdo, P. Pereira-Almao and C.E. Scott, *J. Nanotechnol.*, **2016**, 1 (2016); https://doi.org/10.1155/2016/3752484.
25. Y. Ni, X. Ge, Z. Zhang, H. Liu, Z. Zhu and Q. Ye, *Mater. Res. Bull.*, **36**, 2383 (2001); https://doi.org/10.1016/S0025-5408(01)00739-5.
26. S. Thirumalairajan, K. Girija, N.Y. Hebalkar, D. Mangalaraj, C. Viswanathan and N. Ponpandian, *RSC Adv.*, **3**, 7549 (2013); https://doi.org/10.1039/c3ra00006k.
27. F.J. Manjon and I.U. Tiqinyanu, Springer Series in Materials Science, vol. 189 (2014).
28. M.Y. Arsent'ev, N.Y. Koval'ko, A.V. Shmigel', P.A. Tikhonov and M.V. Kalinina, *Glass Phys. Chem.*, **43**, 376 (2017); https://doi.org/10.1134/S1087659617040022.
29. G. Blasse, *Philip Tech. Rev*., **28**, No. 1, pp. 23-30 (1967).